Syntheses and Characterizations of Four Organically Templated One-Dimensional Molybdenum Compounds including the First Inorganic−Organic Mixed-Anion Structures in the Mo/X/O (X = As, P) System

Ming-Yuan Lee and Sue-Lein Wang*

Department of Chemistry, National Tsing Hua University, Hsinchu, Taiwan 300

Received June 9, 1999. Revised Manuscript Received September 13, 1999

Four new organically templated molybdenum compounds, $(C_4H_{12}N_2)[MoO_2(H_2AsO_4)(AsO_4)]$ (**1**), $(C_4H_{12}N_2)[MoO_2(H_2PO_4)(PO_4)]\cdot H_2O$ (**2**), $(C_4H_{12}N_2)[MoO_2(C_2O_4)(HAsO_4)]$ (**3**), and $(C_6H_{14}N_2)_3[(MoO_2)_4(C_2O_4)_4(H_2PO_4)_2]\cdot 8.5H_2O$ (**4**), have been prepared under mild hydrothermal conditions and characterized by single-crystal X-ray diffraction and thermogravimetric (TG) analysis. All four structures are one-dimensional and contain diprotonated amine cations. The first three compounds are the first organically templated chain structures in the $Mo^{VI}/X/O$ (X = As, P) lattices; **3** and **4** are the first inorganic−organic mixed anion materials in the molybdenum arsenate and phosphate systems, respectively. Crystal data: **1**, monoclinic, $P2_1/n$, a =13.4544(8) Å, b = 6.5648(4) Å, c = 14.6312(8) Å, β = 107.522(1)°, Z = 4; **2**, triclinic, P-1, a = 6.4249(3) Å, b = 8.6860(4) Å, c = 12.4506(6) Å, α = 80.539(1)°, β = 75.140(1)°, γ = 70.161(1)°, Z = 2; **3**, monoclinic, $P2_1/n$, a = 6.4577(2) Å, b = 13.0135(3) Å, c = 15.3606(2) Å, β = 93.199(1)°, Z = 4; **4**, triclinic, P-1, a = 8.6384(1) Å, b = 17.7583(3) Å, c = 18.1172(3) Å, α = 97.979(1)°, β = 102.441(1)°, γ = 98.830(1)°, Z = 2. Both crystals of **1** and **2** contain the double $[Mo_2X_2O_{12}(H_2XO_4)]\infty$ ribbon, which can be derived from that of $VO(HPO_4)\cdot 4H_2O$. Introduction of oxalate anions into the reaction results in **3** and **4**, which contain unusual $[MoAsO_6(C_2O_4)]\infty$ and $[Mo_2PO_8(C_2O_4)_2]\infty$ chains, respectively. According to the results of TG and DT analyses, the structural motifs of **1**, **3**, and **4** are thermally stable up to ∼250 °C.

Introduction

Recently considerable attention has been focused on the organically templated metal phosphates because of their rich structural chemistry and potential applications in heterogeneous catalysis, adsorption, and ion exchange.[1−4] By combining the hydrothermal techniques with organic structure-directing templates, a variety of interesting open-framework transition-metal phosphates[5−10] can be prepared. For example, the chiral double helixlike vanadyl (IV) compound $[(CH_3)_2NH_2]K_4[V_{10}O_{10}(H_2O)_2(OH)_4(PO_4)_7]\cdot 4H_2O$[11] contains enormous cavities, and the novel structure of the iron(III) phosphate $[H_3N(CH_2)_3NH_3]_2[Fe_4(OH)_3(HPO_4)_2(PO_4)_3]\cdot xH_2O$[12] possesses large tunnels with 20-ring windows. In these structures, the cationic organic amine is occluded within an anionic inorganic framework. Recent reports indicate that microporous structures can be prepared by exploiting appropriate metal centers linked through suitable multidentate organic ligands.[13−16] This approach makes possible the rational design and synthesis of coordination polymers with potentially interesting properties. To combine the robustness of the inorganic framework with the greater chemical flexibility of the organic ligands, we previously incorporated both inorganic and organic anions into the structure to provide a new route to open-framework materials and successfully prepared two iron phosphatooxalates.[17] According to a literature search, other than the three iron compounds $(C_4H_{12}N_2)[Fe_4(C_2O_4)_3(HPO_4)_2]$, $(C_4H_{12}N_2)[Fe_2(C_2O_4)(HPO_4)_3]$,[17] and $Fe_4(PO_4)_2(C_2O_4)(H_2O)_2$,[18] neither other transition-metal phosphatooxalates[19−22] nor arsenatooxalates have been

(1) *Eur. J. Solid State Inor. Chem*. **1991**, *28* (special issue).
(2) Haushalter, R. C.; Mundi, L. A. *Chem. Mater*. **1992**, *4*, 31.
(3) Bu, X.; Feng, P.; Stucky, G. D. *Science* **1997**, *278*, 2080.
(4) Barrer, R. M. *Hydrothermal Chemistry of Zeolites*; Academic Press: New York, 1982.
(5) Lii, K. H.; Huang, Y. F.; Zima, V.; Huang, C. Y.; Lin, H. M.; Jiang, Y. C.; Liao, F. L.; Wang, S. L. *Chem. Mater*. **1998**, *10*, 2599.
(6) Lii, K. H.; Huang, Y. F. *Inorg. Chem*. **1999**, *38*, 1348.
(7) Huang, C. Y.; Wang, S. L.; Lii, K. H. *J. Porous Mater*. **1998**, *5*, 147.
(8) Lin, H. M.; Lii, K. H. *Inorg. Chem*. **1998**, *37*, 4220.
(9) Zima, V.; Lii, K. H.; Nguyen, N.; Ducouret, A. *Chem. Mater*. **1998**, *10*, 1914.
(10) Lii, K. H.; Huang, Y. F. *Chem. Commun*. **1997**, *14*, 1311.
(11) Soghomonian, V.; Chen, Q.; Haushalter, R. C.; Zubieta, J.; O'Connor, C. J. *Science* **1993**, *259*, 1596.
(12) Lii, K. H.; Huang, Y. F. *Chem. Commun*. **1997**, *9*, 839.
(13) Yaghi, O. M.; Li, G.; Li, H. *Nature* **1995**, *378*, 703.
(14) Gutsshke, S. O. H.; Molinier, M.; Powell, A. K.; Winpenny, R. E. P.; Wood, P. T. *J. Chem. Soc., Chem. Commun*. **1996**, 823.
(15) Abrahams, B. F.; Hoskins, B. F.; Michail, D. M.; Robson, R. *Nature* **1994**, *369*, 727.
(16) Macgillivray, L. R.; Subramanian, S.; Zaworotko, M. J. *J. Chem. Soc., Chem. Commun*. **1994**, 1325.
(17) Lin, H. M.; Lii, K. H.; Jiang, Y. C.; Wang, S. L. *Chem. Mater*. **1999**, *11*, 519.
(18) Lethbridge, Z.; Lightfoot, P. *J. Solid State Chem*. **1999**, *143*, 58.
(19) There are three non-transition-metal phosphatooxalates that were reported, please refer to the next three papers.
(20) Huang, Y. F.; Lii, K. H. J. *Chem. Soc. Dalton Trans*. **1998**, 4085.
(21) Natarajan, S. *J. Solid State Chem*. **1998**, *139*, 200.
(22) Lightfoot, P.; Lethbridge, Z.; Morris, R. E.; Wragg, D. S.; Wright, P. A. *J. Solid State Chem*. **1999**, *143*, 74.

10.1021/cm990370q CCC: $18.00
Published on Web 11/10/1999

Table 1. Crystallographic Data for Compounds 1−4

	1	2	3	4
formula	$C_4H_{14}As_2MoN_2O_{10}$	$C_4H_{16}MoN_2O_{11}P_2$	$C_6H_{13}AsMoN_2O_{10}$	$C_{26}H_{63}Mo_4N_6O_{40.5}P_2$
fw	495.95	426.07	444.04	1553.53
space group	$P2_1/n$	$P-1$	$P2_1/n$	$P-1$
a, Å	13.4544(8)	6.4249(3)	6.4577(2)	8.6384(1)
b, Å	6.5648(4)	8.6860(4)	13.0135(3)	17.7583(3)
c, Å	14.6312(8)	12.4506(6)	15.3606(2)	18.1172(3)
α,°		80.539(1)		97.979(1)
β,°	107.522(1)	75.140(1)	93.199(1)	102.441(1)
γ,°		70.161(1)		98.830(1)
volume, Å^3	1232.4(1)	629.44(5)	1288.85(5)	2638.92(6)
Z	4	2	4	2
D_{calcd}, g cm^{-3}	2.673	2.248	2.288	1.955
μ, mm^{-1}	6.446	1.358	3.619	1.101
T, °C	22	22	22	22
λ, Å	0.71073	0.71073	0.71073	0.71073
R_1[a]	0.0362	0.0375	0.0604	0.0352
wR_2[b]	0.1002	0.0941	0.1548	0.0804

[a] $R_1 = \sum||F_o| - |F_c||/\sum|F_o|$. [b] $wR_2 = [\sum w(|F_o|^2 - |F_c|^2)^2]/\sum w(|F_o|^2)^2]^{1/2}$, $w = [\sigma 2(F_o^2) + 0.0503P]^2 + 2.9686P]$ for **1**, and $w = [\sigma^2(F_o^2) + 0.0506P]^2 + 2.2596P]$ for **2**, $w = [\sigma^2(F_o^2) + 0.0407P]^2 + 17.6832P]$ for **3**, and $w = [\sigma 2(F_o^2) + 0.0289P]^2 + 6.31P]$ for **4**, where $P = (F_o^2 + 2F_c^2)/3$.

reported so far. To exploit more possibilities, we have extended our investigations into the molybdenum phosphate and arsenate systems. Four new organically templated one-dimensional structures including three Mo(VI) and one Mo(V) materials have thus been prepared. The first two, $(C_4H_{12}N_2)[MoO_2(H_2AsO_4)(AsO_4)]$ (**1**) and $(C_4H_{12}N_2)[MoO_2(H_2PO_4)(PO_4)]\cdot H_2O$ (**2**), were hydrothermally synthesized using organic amine as a template. The latter two, $(C_4H_{12}N_2)[MoO_2(C_2O_4)(HAsO_4)]$ (**3**) and $(C_6H_{14}N_2)_3[(MoO_2)_4(C_2O_4)_4(H_2PO_4)_2]\cdot 8.5H_2O$ (**4**), were prepared by employing both oxalic acid and organic amine as structure-directing reagents. They are the first members in the molybdenum arsenato- and phosphatooxalate systems. We report herein the syntheses, structures, and structural relationships among the four new materials. Thermogravimetric studies of **1**, **3**, and **4** are presented as well.

Experimental Section

Synthesis. Typical hydrothermal reactions were carried out in Teflon-lined digestion bombs with an internal volume of 23 mL under autogenous pressure by heating the reaction mixtures at 160 °C for 3 days followed by slow cooling at 5 °C h^{-1} to room temperature. Needle-shaped, colorless crystals of **1** were obtained from a reaction mixture of piperazine (2.7 mmol), MoO_3 (1.8 mmol), H_3AsO_4 (6 mmol), and 8.8 mL of 50% *n*-butanol in H_2O. The product contained nearly a single phase of **1**. Attempts to prepare its phosphate analogue by a direct replacement of arsenic acid with phosphoric acid in the above reaction did not succeed. After careful scrutiny, solvent effect was found to play an important role in the hydrothermal crystallization of our desired phosphate. By raising the concentration of *n*-butanol in the solvent system, colorless, needlelike crystals of **2** could be isolated. Finally, a product containing **2** as a major phase was obtained by using 100% *n*-butanol as the solvent. However, most of the crystals of **2** were contaminated by unknown white powders that could not completely be removed. Efforts to separate adequate amounts of **2** for measurements other than single-crystal X-ray diffraction have not been achieved.

Preparation of **3** was straightforward by introducing 9 mmol of $H_2C_2O_4\cdot 2H_2O$ into the same reaction solution as that for the preparation of **1**. Despite the drastic change in pH of the starting solution (decreased from 2.38 to 0.65), colorless, needle-shaped crystals of **3** were obtained as a major phase. In contrast, its phosphate analogue could not be prepared with piperazine as a template. After many trials, reddish tabular crystals of **4** were obtained by substituting 1,4-diazabicyclo-[2,2,2]octane (DABCO) for piperazine in the above reaction. An optimum condition for the preparation of **4** was achieved by decreasing the amount of MoO_3 to 1.2 mmol. The product contained a nearly single phase of **4**, as indicated by its powder X-ray diffraction pattern.

Elemental analysis was performed on three materials and confirmed the amount of protonated piperazine in **1** and **3** and DABCO in **4**. Anal. Found for **1**: C, 9.52%; N, 5.69%; H, 3.02%. Calcd: C, 9.69%; N, 5.65%; H, 2.85%. Anal. Found for **3**: C, 16.63%; N, 6.40%; H, 3.10%. Calcd: C, 16.23%; N, 6.31%; H, 2.95%. Anal. Found for **4**: C, 20.04%; N, 5.60%; H, 4.05%. Calcd: C, 20.10%; N, 5.41%; H, 4.09%. Thermogravimetric measurements using a Seiko TGA/DTA 300 thermal analyzer were performed on powder samples of **1**, **3**, and **4** in flowing N_2 with a heating rate of 10 °C min^{-1}.

Single-Crystal X-ray Structure Analysis. The structures of all four compounds were determined by single-crystal X-ray diffraction methods. Typical procedures, for **1** as an example, are given in the following. A needlelike crystal of dimensions 0.02 × 0.035 × 0.40 mm^3 of **1** was selected for indexing and intensity data collection on a Siemens Smart-CCD diffractometer equipped with a normal focus, 3 KW sealed-tube X-ray source (λ = 0.71073 Å). Intensity data were collected in 1271 frames with increasing ω (width of 0.3° per frame). Unit cell dimensions were determined by a least-squares fit of 5094 reflections. The intensity data was corrected for L_p and absorption effects. The number of measured and observed reflections ($I_{obs} > 3\ \sigma_I$) are 7285 and 6142, respectively. Absorption correction was applied based on symmetry-equivalent reflections using the *SADABS* program.[23] On the basis of systematic absences and statistics of intensity distribution, the space group was determined to be $P2_1/n$. The structure was solved by direct methods: the Mo, As, and a few O atoms with the remaining non-hydrogen atoms being found from successive Fourier difference maps. The results of bond-valence sum calculations[24,25] were used to identify the two hydroxooxygen atoms, O(2) and O(4). Most of the hydrogen atoms could be located from Fourier difference maps and calculated at the final stage of structure refinements. The final cycle of refinement, including the atomic coordinates and anisotropic thermal parameters for all non-hydrogen atoms and fixed atomic coordinates and isotropic thermal parameters for the hydrogen atoms, converged at $R_1 = 0.036$ and $wR_2 = 0.100$ for 2318 unique reflections. In the final difference map

(23) Sheldrick, G. M. *SADABS*; Siemens Analytical X-ray Instrument Division: Madison, WI, 1995.
(24) Brown, I. D.; Altermann, D. *Acta Crystallogr.* **1985**, *B41*, 244.
(25) Brown, I. D.; Wu, K. K. *Acta Crystallogr.* **1976**, *B32*, 1957.

Table 2. Atomic Coordinates and Thermal Parameters (Å²) for 1−4

atom	*x*/*a*	*y*/*b*	*z*/*c*	U_{eq}[a]	atom	*x*/*a*	*y*/*b*	*z*/*c*	U_{eq}[a]
				1					
Mo(1)	0.8575(1)	0.5437(1)	0.1913(1)	0.010(1)	O(8)	0.7860(3)	0.0609(5)	0.0427(2)	0.021(1)
As(1)	1.1335(1)	0.5335(1)	0.2963(1)	0.013(1)	O(9)	0.7277(3)	0.5389(5)	0.1290(3)	0.021(1)
As(2)	0.7956(1)	0.0500(1)	0.1585(1)	0.010(1)	O(10)	0.9153(3)	0.5465(5)	0.1023(3)	0.022(1)
O(1)	1.0103(3)	0.5526(5)	0.2987(3)	0.017(1)	N(1)	1.0634(3)	0.8229(6)	0.0357(3)	0.018(1)
O(2)	1.1621(3)	0.2784(6)	0.3116(3)	0.029(1)	N(2)	0.5256(3)	0.3561(6)	0.0766(3)	0.019(1)
O(3)	1.1618(3)	0.6257(6)	0.2031(3)	0.023(1)	C(1)	1.0567(4)	0.9928(8)	0.1008(4)	0.020(1)
O(4)	1.2048(3)	0.6597(6)	0.3962(3)	0.028(1)	C(2)	0.9639(4)	0.8087(8)	−0.0467(4)	0.023(1)
O(5)	0.8720(2)	0.2455(5)	0.2167(2)	0.016(1)	C(3)	0.4588(4)	0.5368(7)	0.0792(4)	0.020(1)
O(6)	0.6770(3)	0.0519(5)	0.1729(2)	0.015(1)	C(4)	0.5153(4)	0.2895(7)	−0.0233(3)	0.022(1)
O(7)	0.8673(2)	−1.525(5)	0.2130(2)	0.016(1)					
				2					
Mo(1)	0.2055(1)	0.4493(1)	0.1513(1)	0.013(1)	O(8)	−0.4249(5)	0.6440(4)	0.2263(3)	0.020(1)
P(1)	0.3044(2)	0.0682(1)	0.2962(1)	0.017(1)	O(9)	0.1352(6)	0.6470(4)	0.0954(3)	0.022(1)
P(2)	−0.3267(2)	0.5366(1)	0.1286(1)	0.012(1)	O(10)	0.1286(6)	0.4738(4)	0.2895(3)	0.022(1)
O(1)	0.2922(5)	0.1845(4)	0.1894(2)	0.017(1)	OW	0.1252(6)	0.1502(5)	0.5838(3)	0.030(1)
O(2)	0.0857(6)	0.1443(4)	0.3861(3)	0.024(1)	N(1)	0.3106(7)	0.5618(5)	0.5891(3)	0.023(1)
O(3)	0.5121(6)	0.0319(5)	0.3388(3)	0.033(1)	N(2)	0.0748(7)	1.1016(5)	0.0505(3)	0.019(1)
O(4)	0.2658(6)	−0.0903(4)	0.2701(3)	0.026(1)	C(1)	0.2904(8)	0.4736(7)	0.5008(4)	0.028(1)
O(5)	−0.0897(5)	0.4184(4)	0.1423(2)	0.016(1)	C(2)	0.5167(10)	0.3512(6)	0.4562(4)	0.030(1)
O(6)	−0.3141(5)	0.6389(4)	0.0163(2)	0.017(1)	C(3)	−0.1116(8)	1.0358(6)	0.1155(4)	0.022(1)
O(7)	−0.4677(5)	0.4183(4)	0.1367(3)	0.018(1)	C(4)	−0.2364(8)	1.0069(6)	0.0363(4)	0.024(1)
				3					
Mo(1)	0.7797(1)	0.2398(1)	0.1301(1)	0.030(1)	O(9)	0.749(1)	0.5124(6)	−0.0223(6)	0.043(2)
As(1)	0.2634(2)	0.2242(1)	0.0526(1)	0.030(1)	N(1)	0.797(2)	0.0719(7)	0.8885(6)	0.035(2)
O(1)	0.480(1))	0.2495(6)	0.1191(5)	0.041(2)	N(2)	0.700(2)	0.0380(7)	0.7063(6))	0.035(2)
O(2)	0.230(2))	0.1074(6)	0.0227(6)	0.051(2)	C(1)	0.577(2)	0.074(1)	0.8528(8)	0.042(3)
O(3)	0.082(2)	0.2703(6)	0.1181(5)	0.035(2)	C(2)	0.551(2)	0.0079(9)	0.7720(8)	0.043(3)
O(4)	0.272(1))	0.3005(6)	−0.0369(5)	0.043(2)	C(3)	0.919(2)	0.0323(9)	0.7420(8)	0.040(3)
O(5)	0.796(1)	0.2719(7))	0.2371(5)	0.044(2)	C(4)	0.950(2)	0.1006(9)	0.8221(8)	0.040(3)
O(6)	0.771(1)	0.2450(5)	−0.0105(5)	0.034(2)	C(5)	0.755(2)	0.4260(8)	0.0100(7)	0.030(2)
O(7)	0.761(1)	0.4044(5)	0.0911(5)	0.034(2)	C(6)	0.769(2)	0.3326(8)	−0.0510(8)	0.032(2)
O(8)	0.802(1)	0.1109(6)	0.1268(6)	0.049(2)					
				4					
Mo(1)	0.3000(1)	0.1826(1)	0.1641(1)	0.020(1)	O(35)	−0.1834(5)	0.1186(3)	0.0031(2)	0.056(1)
Mo(2)	0.0821(1)	0.2511(1)	0.2038(1)	0.020(1)	O(36)	0.7111(5)	0.8393(3)	0.5135(2)	0.063(1)
Mo(3)	0.2588(1)	0.8170(1)	0.3339(1)	0.021(1)	O(37)	0.1956(6)	1.0602(3)	0.3481(3)	0.063(1)
Mo(4)	0.4779(1)	0.7461(1)	0.2997(1)	0.021(1)	O(38)	0.3779(8)	0.6763(5)	0.0571(4)	0.122(3)
P(1)	−0.3242(2)	0.2437(1)	0.1305(1)	0.029(1)	O(39)	0.4173(18)	0.5533(9)	0.0977(10)	0.143(6)
P(2)	0.8882(2)	0.7574(1)	0.3741(1)	0.029(1)	O(40)	0.0914(11)	−0.0398(5)	0.1441(5)	0.157(3)
O(1)	−0.1688(4)	0.2267(2)	0.1743(2)	0.033(1)	O(41)	1.1003(9)	0.3851(5)	0.4309(5)	0.133(3)
O(2)	−0.4582(4)	0.2178(2)	0.1665(2)	0.038(1)	C(1)	0.0217(6)	0.3871(3)	0.1267(3)	0.028(1)
O(3)	−0.3037(5)	0.3325(2)	0.1309(3)	0.057(1)	C(2)	0.0336(6)	0.4144(3)	0.2116(3)	0.029(1)
O(4)	−0.3646(5)	0.2054(3)	0.0454(2)	0.054(1)	C(3)	0.5261(6)	0.5831(3)	0.2978(3)	0.032(1)
O(5)	0.7287(4)	0.7703(2)	0.3303(2)	0.033(1)	C(4)	0.5416(6)	0.6138(3)	0.3837(3)	0.031(1)
O(6)	0.8705(5)	0.6704(3)	0.3778(3)	0.065(1)	C(5)	0.2962(6)	0.8563(3)	0.5042(3)	0.031(1)
O(7)	1.0184(4)	0.7812(2)	0.3345(2)	0.041(1)	C(6)	0.2752(7)	0.9315(3)	0.4752(3)	0.034(1)
O(8)	0.9326(5)	0.8024(3)	0.4567(3)	0.075(2)	C(7)	0.2959(6)	0.0820(3)	0.0171(3)	0.031(1)
O(9)	0.0670(4)	0.1585(2)	0.1310(2)	0.026(1)	C(8)	0.2779(6)	0.1604(3)	−0.0062(3)	0.029(1)
O(10)	0.3066(4)	0.2894(2)	0.2052(2)	0.025(1)	N(1)	0.6480(6)	0.2906(2)	0.4114(2)	0.036(1)
O(11)	0.3036(4)	0.0799(2)	0.0878(2)	0.031(1)	N(2)	0.6299(6)	0.4236(2)	0.3894(3)	0.037(1)
O(12)	0.2771(4)	0.2133(2)	0.0478(2)	0.027(1)	C(9)	0.4750(7)	0.2987(3)	0.3976(3)	0.041(1)
O(13)	0.3467(4)	0.1375(2)	0.2398(2)	0.032(1)	C(10)	0.4662(7)	0.3817(3)	0.3873(4)	0.043(1)
O(14)	0.0688(4)	0.3659(2)	0.2553(2)	0.030(1)	C(11)	0.7388(7)	0.4284(3)	0.4662(4)	0.046(2)
O(15)	0.0371(4)	0.3168(2)	0.1095(2)	0.027(1)	C(12)	0.7439(7)	0.3466(3)	0.4818(3)	0.040(1)
O(16)	0.0913(4)	0.2260(2)	0.2908(2)	0.032(1)	C(13)	0.7126(8)	0.3038(4)	0.3431(3)	0.046(2)
O(17)	0.4921(4)	0.8419(2)	0.3670(2)	0.025(1)	C(14)	0.6936(9)	0.3839(4)	0.3275(4)	0.057(2)
O(18)	0.2540(4)	0.7086(2)	0.2994(2)	0.027(1)	N(3)	−0.0885(6)	0.5733(3)	0.1201(3)	0.038(1)
O(19)	0.2555(4)	0.9258(2)	0.4021(2)	0.032(1)	N(4)	−0.1709(6)	0.6950(3)	0.0884(3)	0.044(1)
O(20)	0.2893(4)	0.7987(2)	0.4540(2)	0.028(1)	C(15)	0.0070(8)	0.7014(4)	0.0943(4)	0.055(2)
O(21)	0.2124(4)	0.8573(2)	0.2552(2)	0.035(1)	C(16)	0.0528(7)	0.6254(4)	0.1087(4)	0.045(2)
O(22)	0.4926(4)	0.6302(2)	0.2527(2)	0.033(1)	C(17)	−0.2211(7)	0.5554(4)	0.0482(4)	0.051(2)
O(23)	0.5217(4)	0.6837(2)	0.3967(2)	0.029(1)	C(18)	−0.2598(7)	0.6305(4)	0.0255(3)	0.046(2)
O(24)	0.4706(4)	0.7676(2)	0.2112(2)	0.034(1)	C(19)	−0.1460(8)	0.6124(4)	0.1856(3)	0.054(2)
O(25)	0.0000(5)	0.4329(2)	0.0820(2)	0.045(1)	C(20)	−0.2100(9)	0.6817(4)	0.1625(3)	0.057(2)
O(26)	0.0094(5)	0.4794(2)	0.2330(2)	0.049(1)	N(5)	0.2819(6)	0.9778(2)	0.6807(3)	0.038(1)
O(27)	0.5480(6)	0.5170(2)	0.2783(2)	0.052(1)	N(6)	0.2556(6)	1.0349(3)	0.8097(3)	0.039(1)
O(28)	0.5703(5)	0.5717(2)	0.4305(2)	0.047(1)	C(21)	0.1987(8)	0.9158(3)	0.7146(4)	0.053(2)
O(29)	0.3198(5)	0.8560(2)	0.5746(2)	0.041(1)	C(22)	0.1714(9)	0.9513(3)	0.7912(4)	0.057(2)
O(30)	0.2750(6)	0.9897(2)	0.5199(2)	0.064(1)	C(23)	0.4303(8)	1.0414(4)	0.8119(4)	0.055(2)
O(31)	0.2978(5)	0.0268(2)	−0.0316(2)	0.050(1)	C(24)	0.4466(7)	1.0104(4)	0.7314(4)	0.050(2)
O(32)	0.2610(5)	0.1670(2)	−0.0748(2)	0.044(1)	C(25)	0.1865(7)	1.0406(3)	0.6727(3)	0.041(1)
O(33)	0.0970(4)	0.5940(2)	0.3591(2)	0.038(1)	C(26)	0.1804(8)	1.0783(3)	0.7523(4)	0.045(2)
O(34)	−0.5354(5)	0.4047(2)	0.1446(2)	0.044(1)					

[a] U_{eq} is defined as one−third of the trace of the orthogonalized U_{ij} tensor.

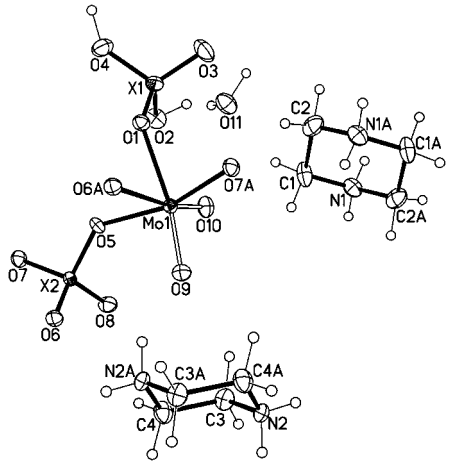

Figure 1. Asymmetric unit of $(C_4H_{12}N_2)[MoO_2(H_2XO_4)(XO_4)]$ (X = As for **1**, and X = P for **2**), showing the atom-labeling scheme and 50% thermal ellipsoids. Open bonds indicate the Mo═O groups.

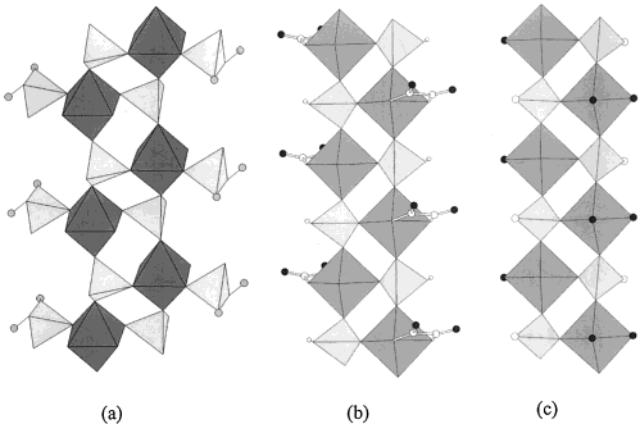

Figure 2. Section of the infinite chain in the structures of (a) **1** and **2**, (b) $(C_4H_{12}N_2)[VO(C_2O_4)HAsO_4]$, and (c) $VO(HPO_4)\cdot 4H_2O$. Black dots in the plot of part c represent coordination water molecules.

the highest peak was 0.91 eÅ^{-3} and the deepest hole −1.32 eÅ^{-3}. Corrections for secondary extinction and anomalous dispersion were applied. Neutral-atom scattering factors for all atoms were taken from the standard sources. All calculations were performed by using *SHELXTL* programs.[26]

Results and Discussion

Crystallographic data are listed in Table 1. The atomic coordinates and the bond lengths and bond valence sums are given in Tables 2 and 3, respectively. Bond-valence calculations[24,25] clearly indicate that **1**−**3** are Mo^{6+} and **4** is a Mo^{5+} species.

Both structures of **1** and **2** are composed of the negatively charged double $[Mo_2X_2O_{12}(H_2XO_4)_2]_8$ (X = As or P) ribbons and piperazinium dications. In addition, **2** contains one lattice water molecule per formula in the crystal. An asymmetric unit of the structure is depicted in Figure 1, and a section of the double ribbon is shown in Figure 2a. The ribbon is topologically similar to that of the vanadyl(IV) compounds $(C_4H_{12}N_2)[(VO)(C_2O_4)$-

(26) Sheldrick, G. M. *SHELXTL*, programs, ver. 5.1; Bruker AXS, 1998.

Table 3. Selected Bond Lengths (Å) and Bond Valence Sums (∑s) for 1−4

	1		
Mo(1)−O(1)	2.181(3)	Mo(1)−O(5)	1.992(3)
Mo(1)−O(6)[a]	2.173(3)	Mo(1)−O(7)[b]	2.017(3)
Mo(1)−O(9)	1.711(4)	Mo(1)−O(10)	1.705(4)
∑s[Mo(1)−O] = 5.995			
As(1)−O(1)	1.672(3)	As(1)−O(2)	1.718(4)
As(1)−O(3)	1.639(3)	As(1)−O(4)	1.703(4)
∑s[As(1)−O] = 5.003			
As(2)−O(5)	1.703(3)	As(2)−O(6)	1.671(3)
As(2)−O(7)	1.695(3)	As(2)−O(8)	1.661(3)
∑s[As(2)−O] = 5.024			
O(2)−H(1)	1.043(3)	O(4)−H(2)	0.916(4)
N(1)−H(3)	1.030(4)		
N(2)−H(4)	0.951(4)	N(2)−H(5)	1.025(4)
	2		
Mo(1)−O(1)	2.175(3)	Mo(1)−O(5)	2.036(3)
Mo(1)−O(6)[c]	2.201(3)	Mo(1)−O(7)[d]	1.988(3)
Mo(1)−O(9)	1.697(3)	Mo(1)−O(10)	1.692(3)
∑s[Mo(1)−O] = 5.983			
P(1)−O(1)	1.534(3)	P(2)−O(2)	1.571(3)
P(1)−O(3)	1.478(4)	P(2)−O(4)	1.576(4)
∑s[P(2)−O] = 4.859			
P(2)−O(5)	1.554(3)	P(2)−O(6)	1.527(3)
P(2)−O(7)	1.561(3)	P(2)−O(8)	1.526(3)
∑s[P(1)−O] = 4.952			
O(2)−H(1)	0.996(3)	O(4)−H(2)	0.994(3)
OW−H(3)	0.965(4)	OW−H(4)	0.883(4)
N(1)−H(13)	0.868(4)	N(2)−H(15	0.903(4)
N(1)−H(14)	1.011(4)	N(2)−H(16)	0.866(4)
	3		
Mo(1)−O(1)	1.938(8)	Mo(1)−O(3)[e]	2.008(7)
Mo(1)−O(5)	1.693(8)	Mo(1)−O(6)	2.158(7)
Mo(1)−O(7)	2.227(7)	Mo(1)−O(8)	1.684(8)
∑s[Mo(1)−O] = 6.194			
As(1)−O(1)	1.718(8)	As(1)−O(2)	1.599(8)
As(1)−O(3)	1.698(7)	As(1)−O(4)	1.699(8)
∑s[As(1)−O] = 5.147			
N(1)−H(10)	1.000(9)	N(2)−H(5)	1.165(9)
N(1)−H(11)	1.180(9)	N(2)−H(7)	1.015(9)
	4		
Mo(1)−Mo(2)	2.5661(5)	Mo(1)−O(2)[f]	2.075(3)
Mo(1)−O(9)	1.933(3)	Mo(1)−O(10)	1.928(3)
Mo(1)−O(11)	2.139(3)	Mo(1)−O(12)	2.225(3)
Mo(1)−O(13)	1.687(3)		
∑s[Mo(1)−O] = 4.937			
Mo(2)−O(1)	2.078(3)	Mo(2)−O(9)	1.928(3)
Mo(2)−O(10)	1.949(3)	Mo(2)−O(14)	2.153(3)
Mo(2)−O(15)	2.200(3)	Mo(2)−O(16)	1.685(3)
∑s[Mo(2)−O] = 4.913			
Mo(3)−Mo(4)	2.5629(5)	Mo(3)−O(7)[g]	2.080(3)
Mo(3)−O(17)	1.936(3)	Mo(3)−O(18)	1.930(3)
Mo(3)−O(19)	2.152(3)	Mo(3)−O(20)	2.209(3)
Mo(3)−O(21)	1.683(3)		
∑s[Mo(3)−O] = 4.936			
Mo(4)−O(5)	2.078(3)	Mo(4)−O(17)	1.921(3)
Mo(4)−O(18)	1.945(3)	Mo(4)−O(22)	2.150(3)
Mo(4)−O(23)	2.202(3)	Mo(4)−O(24)	1.689(3)
∑s[Mo(4)−O] = 4.923			
P(1)−O(1)	1.501(4)	P(1)−O(2)	1.491(3)
P(1)−O(3)		P(1)−O(4)	1.536(4)
∑s[P(1)−O] = 5.180			
P(2)−O(5)	1.502(4)	P(2)−O(6)	1.541(4)
P(2)−O(7)	1.498(4)	P(2)−O(8)	1.534(4)
∑s[P(2)−O] = 5.229			
O(3)−H(1)	0.950(4)	O(4)−H(2)	0.996(4)
O(6)−H(3)	1.019(4)	O(33)−H(6)	0.943(3)
O(34)−H(7)	0.968(4)	O(35)−H(4)	1.119(5)
O(34)−H(8)	0.967(4)	O(35)−H(12)	1.025(4)
O(36)−H(10)	0.895(5)	O(37)−H(5)	0.963(4)
O(36)−H(11)	0.932(4)	O(37)−H(9)	1.078(4)
O(39)−H(13)	1.08(2)	O(41)−H(14)	1.078(8)
N(1)−H(29)	1.030(4)	N(2)−H(15)	0.917(4)
N(3)−H(30)	1.104(4)	N(4)−H(31)	1.149(4)
N(5)−H(32)	1.094(4)	N(6)−H(33)	1.096(4)

[a−f] Symmetry codes: (a) $-x+3/2, y+1/2, -z+1/2$; (b) $x, y+1, z$; (c) $-x, -y+1, -z$; (d) $x+1, y, z$; (e) $x+1, y, z$; (f) $x+1, y, z$; and (g) $x-1, y, z$.

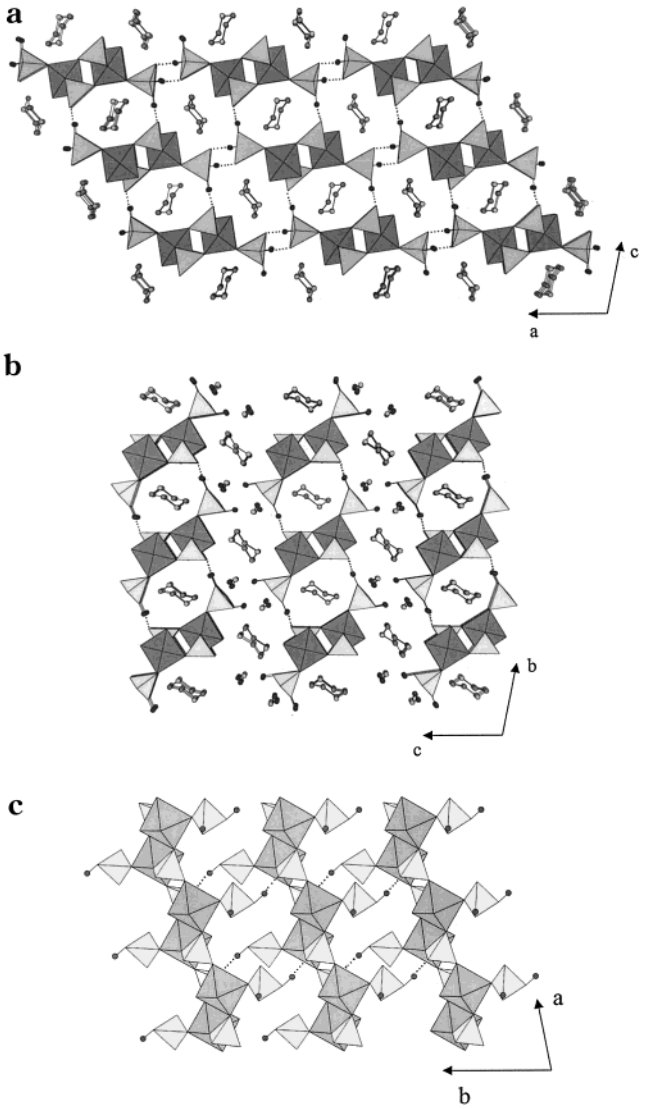

Figure 3. Arrangement of double ribbons in the structures of $(C_4H_{12}N_2)[MoO_2(H_2XO_4)(XO_4)]$. (a) Projection along *b* showing 3D H-bonding network of **1**. (b) Projection along *a* showing the layered feature of **2**. (c) H-bonding layer in the structure of **2**. The In these representations, the darker polyhedra are MoO_6 octahedra, the lighter ones are H_2AsO_4 and AsO_4 tetrahedra, the stippled circles are N and C atoms, and the solid circles are H atoms. Dotted lines indicate interchain H bonds.

$(HXO_4)]$ (X = As or P)[27] (Figure 2b), where oxalate units correspond to the pendent H_2XO_4 tetrahedra in **1** or **2**. These one-dimensional ladderlike motifs are also related to that of $VO(HPO_4)\cdot 4H_2O$[28] (Figure 2c).

In both **1** and **2**, the piperazinium dications possess inversion symmetry and form weak H-bonding to the infinite $[Mo_2X_2O_{12}(H_2XO_4)_2]_8$ ribbons. The anionic double ribbons possess 2_1 screw axis and *n*-glide plane symmetry by themselves. As shown in Figure 3a, each ribbon links to four others via strong H-bonding between the adjacent $H_2As(1)O_4$ tetrahedra along *a* and the H bonds between the nearest $H_2As(1)O_4$ and $As(2)O_4$ tetrahedra along *c*. As a consequence, a three-dimensional H-bonding network with straight tunnels running along *b* is formed. The piperazinium dications are residing in tunnels. In **2**, the ribbons possess merely a center of inversion and each ribbon links to two others via short H bonds between the nearest $H_2P(1)O_4$ and $P(2)O_4$ units along *b* (Figure 3b), resulting in two-dimensional H-bonding "layers" parallel to (001) planes (Figure 3c). As the distance between the two nearest $H_2P(1)O_4$ units in **2** is larger than the corresponding $H_2As(1)O_4$ units in **1** (5.8 vs 5.0 Å), the H_2O molecule located between the $H_2P(1)O_4$ units in the former form bridging H bonds. Relative to **1**, there are no direct H-bonding interactions between interchain $H_2P(1)O_4$ groups in **2**. The connection between adjacent "layers" is therefore through the hydrogen bonds interleaved by H_2O molecules.

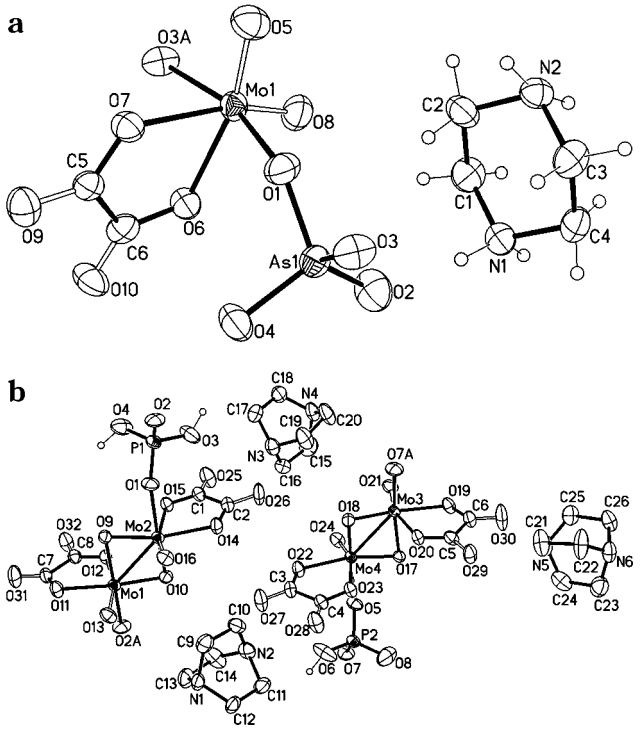

Figure 4. Asymmetric unit in the structure of (a) **3** and (b) **4**.

Crystals of **3** contain diprotonated piperazine cations and anionic $[MoAsO_6(C_2O_4)]\infty$ chains, whereas **4** contains diprotonated DABCO cation and anionic $[Mo_2PO_8(C_2O_4)_2]\infty$ chains. Drawings of asymmetric units in the two structures are given in Figure 4, and the single chains are shown in Figure 5. In both **3** and **4**, oxalate anions coordinate to Mo centers as bidentate ligands. Strong H-bonding exists between oxalate anions and organic cations. The complete H-bonding scheme is given in Table 4. Relative to **1** and **2**, no direct H bonding exists between neighboring chains of **3** and **4**. Nevertheless, the infinite chains are H-bonded into three-dimensional (3D) networks (Figure 6) by extremely short H bonds that are interleaved by organic cations.

An interesting feature of **3** lies in the single $[MoAsO_6(C_2O_4)]_8$ chain (Figure 5a) that may be considered as derived from the double $[Mo_2As_2O_{12}(H_2AsO_4)_2]_8$ ribbon of **1** by the substitution of pendent H_2AsO_4 units for bidentate oxalate groups. The substitution requires breaking half of the Mo−O−P type bonds in the original

(27) Tsai, Y. M.; Wang, S. L.; Huang, C. H.; Lii, K. H. *Inorg. Chem.* **1999**, *38*, 4183.

(28) Leonowicz, M. E.; Johnson, J. W.; Brody, J. F.; Shannon, H. F.; Newsam, J. M. *J. Solid State Chem.* **1985**, *56*, 370.

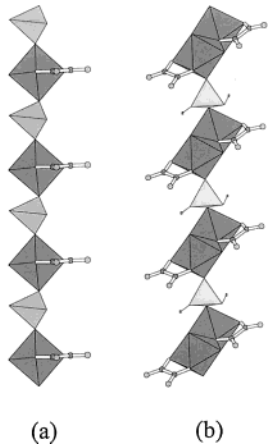

Figure 5. Section of inorganic/organic chains: (a) the $[MoAsO_6(C_2O_4)]\infty$ chain of **3** and (b) the $[Mo_2PO_8(C_2O_4)_2]$ chain of **4**.

Table 4. Hydrogen-Bond Distances (Å) and Angles (deg) for 1−4

		1		
	O − H	H ··· O	O ··· O	N − H ··· O
O(2) − H(1) ··· O(3A)	1.043	1.607	2.633	167.0
O(4) − H(2) ··· O(8B)	0.916	1.639	2.536	166.4
	N − H	H ··· O	N ··· O	N − H ··· O
N(2) − H(4) ··· O(1B)	0.951	1.923	2.832	160.7
	1.025	1.922	2.870	151.2
		2		
	O − H	H ··· O	O ··· O	N − H ··· O
O(2) − H(1) ··· O(11)	0.996	1.619	2.549	153.2
O(4) − H(2) ··· O(8A)	0.994	1.540	2.510	164.4
OW − H(3) ··· O(11B)	0.965	1.684	2.647	175.4
OW − H(4) ··· O(11B)	0.883	1.971	2.851	174.9
	N − H	H ··· O	N ··· O	N − H ··· O
N(1) − H(13) ··· O(2A)	0.868	2.069	2.923	167.1
N(1) − H(14) ··· O(8B)	1.011	1.754	2.764	177.7
N(2) − H(15) ··· O(9A)	0.903	1.989	2.804	148.9
N(2) − H(16) ··· O(1A)	0.866	1.943	2.789	165.3
		3		
	N − H	H ··· O	N ··· O	N − H ··· O
N(1) − H(10) ··· O(2A)	1.000	1.745	2.711	161.4
N(1) − H(11) ··· O(6A)	1.180	1.620	2.744	156.8
N(2) − H(5) ··· O(3B)	1.165	2.093	2.923	125.1
N(2) − H(7) ··· O(10A)	1.015	1.827	2.789	156.8
		4		
	N − H	H ··· O	N ··· O	N − H ··· O
N(1) − H(29) ··· O(29)	1.030	1.692	2.702	166.5
N(2) − H(15) ··· O(28)	0.917	1.999	2.789	143.4
	O − H	H ··· O	O ··· O	N − H ··· O
O(3) − H(1) ··· O(34)	0.950	1.632	2.572	169.3
O(4) − H(2) ··· O(35)	0.996	1.554	2.518	161.7
O(6) − H(3) ··· O(33)	0.943	1.584	2.601	173.1
O(35) −H(4) ··· O(31)	1.119	1.675	2.771	167.0
O(35) −H(12) ··· O(9)	1.025	1.722	2.735	168.1
O(36) −H(11) ··O(37)	0.932	1.862	2.750	158.1
O(39) −H(13) ··O(38)	1.08	1.595	2.735	168.1

chains so that each of the incoming oxalate anions can obtain two coordination sites. After substitution, the double ribbon of **1** is accordingly cleaved into two single $[MoAsO_6(C_2O_4)]\infty$ chains. Despite the source of O^{2-}, the existence of an isolated $[MoXO_8]\infty$ chain[29] has not previously been discovered. **3** not only represents the first molybdenum arsenatooxalate but also the first $[MoXO_8]\infty$ chain structure in molybdenum chemistry.

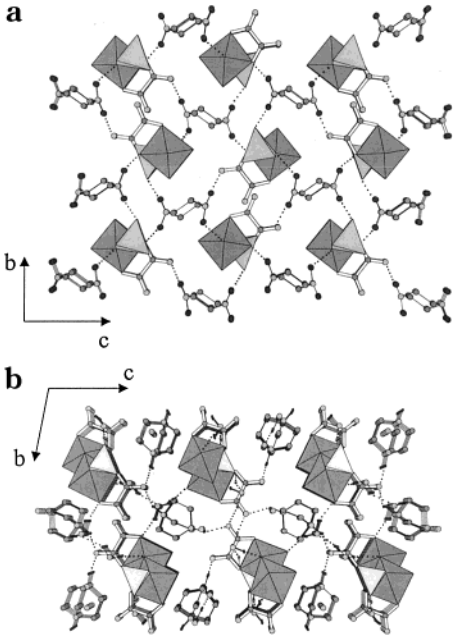

Figure 6. Projection of the single chains in the structures of (a) **3** and (b) **4** along the *a*-axis direction. Connections among chains are through short H bonds interleaved by organic cations in both structures.

An interesting feature of **4** lies in the fact that it is the first inorganic−organic mixed-anion structure in the molybdenum−phosphate system. The single $[Mo_2PO_8(C_2O_4)_2]_8$ chain is composed of tetrahedral H_2PO_4 units and bioctahedral Mo_2O_{10} units in a alternatively corner−shared manner. The pentavalent character of the Mo atoms in the Mo_2O_{10} unit is confirmed by valence calculations.[25] Magnetic susceptibility measurements, which showed **4** to have diamagnetic behavior, corroborated the presence of a Mo−Mo bond between the two Mo^{5+} centers in Mo_2O_{10} units, as well. Within the $[Mo_2PO_8(C_2O_4)_2]\infty$ chains, each of the Mo_2O_{10} dimers is connected to two PO_4 tetrahedra and two oxalate groups and exhibits two free apexes. These two molybdenyl oxygen atoms show a cis configuration with respect to the equatorial plane of the Mo_2O_{10} bioctahedra (Figure 4b). The single chain of **4** is similar to that of **3** in the sense that the bioctahedra of Mo_2O_{10} units in the former correspond to the octahedra of MoO_6 in the latter. Edge-sharing Mo_2O_{10} units were already observed in three Mo(V) phosphates: $Na_3Mo_2P_2O_{11}(OH)\cdot 2H_2O$,[30] β-$K_2(MoO_2)_2P_2O_7$,[31] and $CdMoO_2PO_4$.[32] The short Mo−Mo distance of **4** (2.56 Å) is comparable to those encountered in the other compounds. In addition, the Mo_2O_{10} units have the same configuration as those found in the above-mentioned Na and K compounds.

In the TG/DT analyses, both **1** and **3** showed a thermal stability up to ∼250 °C and completely vaporized beyond 820 °C. As shown in the TG curves in Figure 7, the mass loss for both materials can roughly be

(29) Costentin, G.; Leclaire, A.; Borel, M. M.; Grandin, A.; Raveau, B. *Rev. Inorg. Chem.* **1993**, *13*, 77.
(30) Mundi, L. A.; Haushalter, R. *Inorg. Chem.* **1990**, *29*, 2879.
(31) Guesdon, A.; Leclaire, A.; Borel, M. M.; Grandin, A.; Raveau, B. *J. Solid State Chem.* **1995**, *114*, 481.
(32) Guesdon, A.; Leclaire, A.; Borel, M. M.; Raveau, B. *Solid State Chem.* **1996**, *122*, 343.

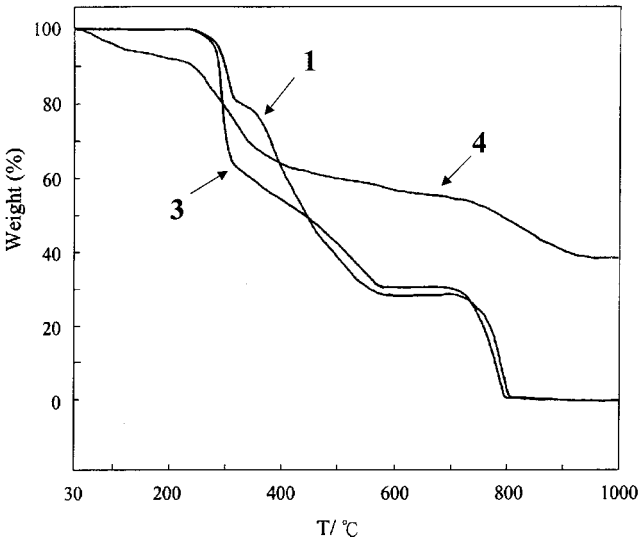

Figure 7. Thermogravimetric curves for **1**, **3**, and **4** in flowing N_2 at 10 °C min^{-1}.

divided into three stages between 250 and 820 °C. In the TG curve of **1**, the first stage, ranging from 250 to ~325 °C, corresponds to dehydration of H_2AsO_4 groups and the removal of piperazine molecules. The second stage, in the region between 325 and ca. 640 °C, should be attributed to further dehydration of the thermal product and decomposition of the arsenate group.[33−35] The total observed mass loss for the first two stages is 67.5% which compares well with the calculated value of 68.17%. The observed mass loss (31.2%) for the sharp fall beyond 700 °C corresponds to the further release of $^1/_2O_2$ (calcd 3.22%) and sublimation of MoO_3 (calcd 29.01%). In the TG curve of **3**, the first stage, from 250 to ca. 320 °C, is attributed to the removal of piperazine molecules and decomposition of oxalate anions. The second stage, in the region between 320 and ca. 600 °C, should correspond to further dehydration of the thermal product and decomposition of the arsenate group. The total observed mass loss for the first two stages can be compared with the calculated value (68.5% vs 67.58%). The observed mass loss (31.5%) for the sharp fall beyond ca.700 °C is due to the sublimation of MoO_3 (calcd 32.42%).

The TG/DT curves of **4** showed that no other components but lattice H_2O molecules were released before 250 °C. A sequential mass loss between ca. 250 and 350 °C should correspond to dehydration of H_2PO_4 groups and the removal of DABCO molecules. The mass loss beyond ca. 350 °C should be attributed to the decomposition of oxalate groups. All of the above steps were not well-resolved from each other. However, the total observed mass loss (57.8%) can be compared well with the calculated value (56.9%) on the basis of the above interpretation.

In conclusion, four new organically templated molybdenum compounds have been synthesized under mild hydrothermal conditions. They adopt three different types of chain structures that are closely related to each other. One-dimensional molybdenum phosphates or arsenates with Mo in the 6+ oxidation state are rare.[36] The discovery of these four new materials are of much significance because they provide the first examples in the organically templated Mo/As/O system (**1** and **3**), the first chain structure in the organically templated Mo^{VI}/P/O system (**2**), the first structure containing an isolated $[MoAsO_8]\infty$ chain (**3**), and the first inorganic−organic mixed-anion materials in the systems of Mo/As/O (**3**) and Mo/P/O (**4**). All of the one-dimensional structures are templated by piperazinium dications except **4**. Until now, this Mo^{5+}-containing species could only be prepared by using DABCO as a template. It is unclear to us why the latter led to the reduction from Mo^{6+} to Mo^{5+}. **4** could not be crystallized in the presence of piperazine as a template, even if Mo metal powder was added into the reactions. As a matter of fact, no other molybdenum compounds with Mo atoms in oxidation states less than +6 could be obtained by including Mo metal as a reactant during this study. Besides the two different amine templates, a solvent effect has been observed to be critical in the crystallization of **2**. The structural variations from **1** and **2** to **3** and **4** are rather interesting. In contrast to the existing iron phosphatooxalates,[17,18] in which oxalate groups bridge inorganic chains or sheets into 3D framework structures, this work demonstrates an opposite example, i.e., that the incorporation of oxalate anions into inorganic double chains results in single chains. The roles assumed by oxalate anions, established by our previous work[17,27] and current studies, are then 2-fold: (i) as a bridging ligand between inorganic anions and (ii) as a terminal ligand coordinated to anionic covalent backbones. It shall be interesting to look for synthetic conditions of 3D open-framework molybdenum phosphato- and arsenato-oxalates. From there, an improved understanding of the particular role of templates may lead to a better designed synthesis of porous structures. Investigations along these lines are in progress.

Acknowledgment. We are grateful to the National Science Council of the Republic of China for support of this work (NSC-88-2113-M007-041).

Supporting Information Available: X-ray crystallographic data including tables of complete crystal data, atomic coordinates, bond distances and angles, and anisotropic thermal parameters for **1**−**4**. This material is available free of charge via the Internet at http://pubs.acs.org.

CM990370Q

(33) Hsu, K. F.; Wang, S. L. *Inorg. Chem.* **1998**, *37*, 3230.
(34) Hsu, K. F.; Wang, S. L. *Inorg. Chem.* **1997**, *36*, 3049.
(35) Wang, S. L.; Hsu, K. F.; Nieh, Y. P. *J. Chem. Soc., Dalton Trans.* **1994**, 1681.
(36) Xu, Y. *Curr. Opin. Solid State Mater. Sci.* **1999**, *4*, 133.